Research Article

Prediction of Normal Bone Anatomy for the Planning of Corrective Osteotomies of Malunited Forearm Bones Using a Three-Dimensional Statistical Shape Model

Flavien Mauler, MD(1), Christoph Langguth, PhD(2), Andreas Schweizer, MD(1), Lazaros Vlachopoulos, MD(3), Tobias Gass, PhD(4), Marcel Lüthi, PhD(2), Philipp Fürnstahl, PhD(3)

(1) Department of Orthopaedics, Balgrist University Hospital, University of Zurich, Zurich, Switzerland
(2) Department of Mathematics and Computer Science, University of Basel, Basel, Switzerland
(3) Computer Assisted Research & Development Group, Balgrist University Hospital, University of Zurich, Zurich, Switzerland
(4) Computer Vision Laboratory, ETH Zurich, Zurich, Switzerland

Corresponding author:
Flavien Mauler
Department of Orthopaedics, Balgrist University Hospital, University of Zurich, Zurich, Switzerland
Phone: +4176 507 50 74
E-mail: flavien.mauler@gmail.com

Running title: Statistical Shape Model of the Forearm Bones

All authors were involved in most aspects of the study including the preparation of the manuscript, as mentioned in the table:

Authors' contributions:
FM, AS, LV, and PF designed the study. FM and PF wrote the manuscript. FM, CL, TG, ML, and PF acquired and processed the data. All authors discussed the results and interpretation of data, and commented the manuscript al all stages.

†This article has been accepted for publication and undergone full peer review but has not been through the copyediting, typesetting, pagination and proofreading process, which may lead to differences between this version and the Version of Record. Please cite this article as doi: [10.1002/jor.23576]

Received 2 September 2016; Revised 22 March 2017; Accepted 29 March 2017
Journal of Orthopaedic Research

DOI 10.1002/jor.23576

ABSTRACT

Corrective osteotomies of the forearm based on 3D computer simulation using contralateral anatomy as a reconstruction template is an approved method. Limitations are existing considerable differences between left and right forearms, and that a healthy contralateral anatomy is required. We evaluated if a computer model, not relying on the contralateral anatomy, may replace the current method by predicting the pre-traumatic healthy shape. A statistical shape model (SSM) was generated from a set of fifty-nine CT scans of healthy forearms, encoding the normal anatomical variations. Three different configurations were simulated to predict the pre-traumatic shape with the SSM (cross-validation). In the first two, only the distal or proximal 50% of the radius were considered as pathological. In a third configuration, the entire radius was assumed to be pathological, only the ulna being intact. Corresponding experiments were performed with the ulna. Accuracy of the prediction was assessed by comparing the predicted bone with the healthy model. For the radius, mean rotation accuracy of the prediction between 2.9±2.2° and 4.0±3.1° in pronation/supination, 0.4±0.3° and 0.6±0.5° in flexion/extension, between 0.5±0.3° and 0.5±0.4° in radial-/ulnarduction. Mean translation accuracy along the same axes between 0.8±0.7 and 1.0±0.8mm, 0.5±0.4 and 0.6±0.4mm, 0.6±0.4 and 0.6±0.5mm, respectively. For the ulna, mean rotation accuracy between 2.4±1.9° and 4.7±3.8° in pronation/supination, 0.3±0.3° and 0.8±0.6° in flexion/extension, 0.3±0.2° and 0.7±0.6° in radial-/ulnarduction. Mean translation accuracy between 0.6±0.4mm and 1.3±0.9mm, 0.4±0.4mm and 0.7±0.5mm, 0.5±0.4mm and 0.8±0.6mm, respectively. This technique provided high accuracy, and may replace the current method, if validated in clinical studies. This article is protected by copyright. All rights reserved

Keywords: Forearm; Osteotomy; Three-Dimensional; Template; Statistical Shape Model

INTRODUCTION

Malunion after fracture of the forearm bones may lead to pain, carpal and distal radioulnar joint instability, osteoarthritis, reduced range of motion and reduced grip strength (1-7). Corrective osteotomy is a surgical method to restore the normal bone anatomy that aims at improving function and reducing pain of the patient (1, 8, 9). Three-dimensional (3D) computer simulation based on computed tomography (CT) reconstructed bone models has proven to be an accurate and reliable method for the assessment of mutli-planar malunions of the forearm (10-17). In the 3D planning approach, bilateral CT scans of both forearms are acquired to generate 3D surface models of the pathological and the contralateral, healthy bone. The contralateral model is then mirrored and used for the quantification of the malunion and the subsequent simulation of the corrective osteotomy on the computer. Although contralateral-based osteotomy planning is an elegant and efficient approach, relying on the contralateral bone has substantial disadvantages. The approach can be applied only to patients which have a healthy contralateral bone, limiting the application to bilateral deformities that are commonly observed (18). Though even if a healthy contralateral bone is available, clinical studies have demonstrated considerable side-to-side differences between the left and right forearm within an individual (19, 20), which, consequently, can introduce errors in the preoperative plan. Moreover, relying on the contralateral CT increases the radiation to which the patient is exposed.

A 3D statistical shape model (SSM), encoding the anatomical variation of normal forearm bones, may have the potential to replace the contralateral-based planning approach by predicting the pre-traumatic healthy shape of the pathological bone. The

purpose of this study was to evaluate how accurately the prediction of the anatomy can be performed with an SSM.

MATERIALS AND METHODS

Institutional review board approval was obtained prior to the start of the study. The SSM was generated from a set of fifty-nine CT scans of healthy right and left forearm bones that were available in our institution. The image data had been acquired using a Philips Brilliance 40 CT device with an axial and in-plane resolution of 1 mm and 0.25x0.25 mm, respectively. Inclusion criteria were patients being eighteen years of age or older, who had undergone a CT scan of a healthy forearm. The segmentation of the forearm bones were performed automatically using a previously validated algorithm (21). 3D triangular surface models were generated from the segmented images using the marching cubes algorithm (22). Based on the 3D bone models a joint SSM of both forearm bones was computed with an in-house developed statistical model building algorithm, described and evaluated in a previous study (23). To eliminate variations due to different pro-supination pose, the pro-supination pose of all the models were normalized with respect to a reference model being in neutral position. This was achieved by separately aligning the ulna and radius using Procrustes alignment (24) to the respective bone in the reference. After alignment and prediction of the individual bone shapes, the bones were transformed back to their initial pose. In summary, the bone position was corrected, the prediction was done in a normalized pose, and then the bones were back-transformed to restore their initial pose.

Prediction and Evaluation

For the evaluation of the predictive power of the SSM, leave-one-out cross validation tests (25) were performed on the entire data set. That means, with respect to the radius experiments, that three regions of different size and location (herein after called configurations; see Fig. 1) of each radius of the data set were predicted by an SSM which was built from all other forearm bones in the database. The forearm which was not included in the SSM generation was used later as a ground-truth for evaluation of the accuracy of the prediction. The first two configurations R_d and R_p aimed at the prediction of only the distal 50% and proximal 50% of the radius, respectively. Although less relevant for osteotomy planning, we were also interested if the entire radius (configuration R_e) can be sufficiently predicted by the SSM. Experiments U_d, U_p and U_e were accordingly performed to predict the distal 50% of the ulna, the proximal 50% of the ulna, and the entire ulna respectively.

For the prediction, a Gaussian process regression method was applied, as described in (26). The main idea is that given the healthy surface regions of the radius and ulna (Fig. 1, green), Gaussian process regression finds the best matching shape to this given region within the set of shapes represented by the model. For example, if predicting region R_d of case 1, the SSM was built using cases 2-59. Thereafter, the (healthy) bone regions R_p and U_e were used by the SSM to predict R_d.

The leave-one-out tests (27) were performed for each of the six configurations R_e, R_d, R_p, U_e, U_d, and U_p and for all of the fifty-nine forearm bones, resulting in a total of 354 tests. For the quantification of the accuracy of the prediction, i.e., the deviation between predicted and original shape, we used two different measurement techniques that have been used previously in studies investigating contralateral differences of bone anatomy

based on 3D models (20, 28-30). In the first technique (30), the model surfaces where discretized as dense point sets (sampled in 1 mm resolution), permitting to determine the distance for a given point on one model surface to the closest point on the other surface. The distance errors were then assessed by calculating mean and Hausdorff distances (29) between all points of the predicted region and the ground-truth bone.

In the second measurement method (20, 28) the difference between ground-truth and the predicted part was measured with a surface-registration method, permitting to quantify the differences between two 3D surfaces in all 6 degrees of freedom (3 translations and 3 rotations) according to an anatomical coordinate system. As illustrated in Fig. 2 for configuration U_e and R_d, the fitted SSM are separated by a simulated osteotomy plan (Fig. 2A and C), and aligned to the ground-truth surface (Fig. 2B and D). The relative transformation (20, 26) of the separated parts between their predicted (Fig. 2A and C) and ground-truth position (Fig. 2B and D) was then used as the error measure. The 3D rotational errors were described by 3 angles around a standardized coordinate system, which origin was set at the level of the osteotomy. The longitudinal axis of each bone (x-axis) corresponds to rotations in the transverse plane (pronation/supination), y-axis in the sagittal plane (flexion/extension) is directed toward the radial styloid for the radius, and parallel to the trochlear notch for the ulna. Z-axis in the frontal plane (ulnar-/radialduction) is perpendicular to the x- and y-axes, as shown in Fig. 3A and B. The 3D translation errors were expressed as a displacement vector with respect to the same coordinate system. The coordinate system was adapted in that way that a positive rotation around the defined axis defined for both sides of the radius and ulna a supination, flexion and radialduction, respectively. The preoperative planning software CASPA (Balgrist CARD AG, Zurich, Switzerland) was used for the simulations and accuracy measurements.

Statistical Analysis

Continuous values were expressed in degrees and millimeters, means and SDs. ANOVA was applied for testing differences in rotation and translation accuracy of the prediction between the anatomical axes for each experiment R_e, R_d, R_p, U_e, U_d, and U_p. Post-hoc analysis was performed by applying Tukey's honest significant difference (HDS) method. A repeated measures ANOVA (within subject: experiments; between subject: axes) was conducted to investigate a difference in the prediction accuracy between R_e, R_d, and R_p. Here, post-hoc analysis was performed with a paired t-test and Bonferroni adjustment. The same tests were applied for the ulna experiments U_e, U_d, and U_p. Paired t-tests were used to evaluate whether the radius or the ulna can be predicted with less error. The significance level was set at $P<0.05$. For graphical visualization, Tukey boxplots were used with the end of the whiskers indicating the 1.5 interquartile range (IQR) of the lower and upper quartile.

RESULTS

Table 1 summarizes the accuracy of the prediction with respect to the average point-to-point distances between predicted and ground-truth model surfaces using the Euclidean and Hausdorff distance error measures. All configurations where only half of a bone was predicted (R_d, R_p, U_d, U_p) had average point-to-point distances below 1 mm. The configurations R_e and U_e had the greatest residual distance errors, with an average Euclidean distances of 1.16 ± 0.28 mm and 1.14 ± 0.19 mm, respectively.

In Table 2, the results of the accuracy evaluation obtained using the surface-registration method are given for each configuration. In Fig. 4 and Fig. 5, the variations of the prediction accuracy based on directed (signed) and undirected (absolute) measurement values, respectively, are displayed by box plots. In all experiments, the statistical tests showed for both the radius and ulna that the prediction error in pronation/supination was significantly greater compared to the one in flexion/extension and radial/ulnar deviation ($P < 0.001$). The prediction error in translation was also significantly greater along the pro-supination axis, but only in configurations R_e, R_d, and U_e, U_d ($P < 0.001$).

Statistical comparison of the prediction accuracy between the different configurations: The shape prediction was less accurate with respect to all 6 degrees of freedom (i.e., 3D rotation and translation) if the region that has to be predicted was larger, i.e., the prediction $R_e$of the entire radius was significantly less accurate ($P < 0.03$) compared to the configurations R_d, and R_p. The same trends were observed for the ulna ($P < 0.04$) except that no significant difference of the prediction error in translation along ulnar-/radialduction direction was observed between the ulna configurations ($P = 0.33$). Comparing the prediction accuracy of the proximal and distal radius (configuration R_d vs. R_p), only the prediction error in rotation around the flexion-extension axis was significantly smaller ($P = 0.03$) for R_p. The prediction of the proximal ulna shape was significantly more accurate ($P < 0.029$) compared to the distal shape (configurations U_d vs. U_p) for all axes of the coordinate system and for both the translation and rotation.

Prediction accuracy of the radius compared to the ulna: The prediction of the distal radius was also significantly better ($P < 0.05$) compared to the distal ulna (experiments R_d vs. U_d), except for the translation along the flexion-extension axis ($P = 0.052$).

Contrary, in the prediction of the proximal parts (experiments R_p vs. U_p) the ulna shape was predictedted more accurately ($P < 0.05$) except for rotation around the flexion/extension axis ($P = 0.3$) and translation along the ulnar-/radialduction axis ($P = 0.38$). If the entire bone was predicted (experiments R_e vs. U_e), a significant difference of the prediction accuracy was observed only in translation along the pro-supination axis where the radius prediction performed better ($P = 0.008$).

DISCUSSION

The treatment of malunited forearm bones remains challenging, particularly due to the complex interaction between the proximal and distal radioulnar joints and the radiocarpal joint. The goal of surgical treatment is to re-establish the function through restoration of the normal anatomy. The currently preferred technique (10, 14, 15, 31), and probably the most reliable one (16), is computer assisted corrective osteotomy based on 3D preoperative planning. State-of-the art approaches still use the healthy contralateral anatomy as a 3D reconstruction template although it was recently shown by Vroemen et al. (20), or earlier by Bindra et al. (32) and Auerbach and Ruff (19), that substantial differences between the left and right forearm bones of an individual can occur. The increased radiation exposure caused by the CT-scanning of the contralateral side is another major limitation, especially in a young population in reproductive age.

The goal of this study was to investigate whether a SSM can be used as a representation of the pre-traumatic bone shape for 3D osteotomy planning. Based on findings of previous studies (33-35) and on our personal experience in performing corrective osteotomies of the forearm, an accuracy of the reduction of 1 mm with respect to the

bone length (ulnar variance), 2° with respect to the angulation (flexion/extension and radial-/ulnarduction), and 5° with respect to torsion are desirable. In the majority of post-traumatic malunion observed clinically only part of the bone shape is deformed. Therefore, we focused on the assessment of the prediction accuracy if only half of the bone is considered to be malunited (configurations R_d, R_p, U_d, U_p). In these experiments, the evaluation based on the distance measured showed that the shape can be predicted within an average accuracy of less than 1 mm with respect to the mean distance error. The SSM performed also better than the contralateral-based planning approach if comparing our results with the left-right differences described in previous studies. In experiments R_d, the present technique shows a mean prediction error in translation of 1.0 mm along the pro-supination axis, and mean errors of 2.9°, 0.6° and 0.5° in rotation around the pro-supination, flexion/extension, and radial-/ulnarduction axes, respectively. For the distal ulna, i.e. the experiments U_d, there was a mean prediction error in translation of 1.3 mm along the pro-supination axis, and mean errors of 4.9°, 0.8° and 0.7° in rotation around the pro-supination, flexion/extension, and radial-/ulnarduction axes, respectively. The model showed a higher error in pro-supination, but in a range of <5°, which does not impact on the forearm rotation (34). Vroemen et al. (20) investigated contralateral differences of healthy forearm bones in 3D. In their scatterplot, they reported a translation asymmetry between the left and right radius of an individual of up to 7.0 mm along the pro-supination axis, 3.5 mm along the flexion/extension-axis, and 1.5 mm along the ulnar-/radialduction-axis. Pointing out the importance of ulnar variance in the restoration of the normal anatomy (33), one can say that our SSM-based approach performs comparably well with respect to the translation error, considering our findings about the maximal translation error along the longitudinal axis of 3.4 mm and 3.6 mm for the radius (R_d) and ulna (U_d),

respectively. Bindra et al. (30) found a mean rotational difference around the pro-/supination axis between paired side-to-side radius of 4.9°. Dumont et al. (32) have also emphasized the importance of the torsional component in radius and ulna malunions. Vroemen et al. (20) studied only the distal radius, and reported a torsional asymmetry between the left and right healthy distal radius of up to 12° for the pro-/supination, while we have observed a maximal error for the distal radius (R_d) of only 10.8° if using the SSM as a reconstruction template. Nevertheless, the prediction of our SSM is less accurate in pro-supination compared to the other anatomical planes.

Less frequently treated by computer assisted osteotomy are, in our experience, deformities where the entire bone is deformed. One application may be treatment of congenital deformities caused by birth defects. Therefore, we were also interested in evaluating the accuracy of our approach if the the entire bone shape must be predicted. Here, we observed higher errors particularilly in pro-supination direction. However, it is obvious that the error around the longitudinal axis is greater compared to the other configurations, because radius and ulna do not have the same torsional twist.

This study is limited by the fact that the SSM method was compared to the current state-of-the-art only by using historical data from previous studies. However, bilateral CT scans of healthy subjects would have been required to conduct a direct comparison of the contralateral anatomy within the same population. Furthermore, the present study did not predict simultaneous both bones deformity, and the possibility of an error accumulation which could happen in this setting could not be tested. Despite this limitation, the novel technique proposed here provided promising results, similar to those reported about the contralateral-based 3D planning technique, which may be sufficiently accurate for the 3D planning of a corrective osteotomy, especially when predicting only the distal or proximal half of the bone. The technique may be also

helpful when the forearm bones of both sides are pathological. Furthermore, the workflow of the preoperative assessment can be simplified, because the contralateral limb is often acquired in a separate radiological examination, which may be weeks after the first consultation.

We strongly believe that the developed method has the potential to replace the current contralateral-based preoperative planning method of corrective osteotomies of the forearm, but further studies are required to evaluate the clinical outcome of corrective osteotomies which are based on 3D preoperative planning using SSM.

ACKNOWLEDGMENTS

This work was partially funded by the Swiss Canton of Zurich, Switzerland through a Highly-Specialized Medicine grant. Andreas Schweizer and Philipp Fürnstahl are both shareholder of the Balgrist CARD AG, a company developing preoperative planning software.

REFERENCES

1. Nagy L, Jankauskas L, Dumont CE. 2008. Correction of forearm malunion guided by the preoperative complaint. Clin Orthop Relat Res 466: 1419-28.

2. Trousdale RT, Linscheid RL. 1995. Operative treatment of malunited fractures of the forearm. J Bone Joint Surg Am 77: 894-902.

3. Cheng HS, Hung LK, Ho PC, Wong J. 2008. An analysis of causes and treatment outcome of chronic wrist pain after distal radial fractures. Hand Surg 13: 1-10.

4. Crisco JJ, Moore DC, Marai GE, et al. 2007. Effects of distal radius malunion on distal radioulnar joint mechanics -an in vivo study. J Orthop Res 25: 547-55.

5. McQueen M, Caspers J. 1988. Colles fracture: does the anatomical result affect the final function? J Bone Joint Surg Br 70: 649-51.

6. Overgaard S, Solgaard S. 1989. Osteoarthritis after Colles' fracture. Orthopedics 12: 413-6.

7. Taleisnik J, Watson HK. 1984. Midcarpal instability caused by malunited fractures of the distal radius. J Hand Surg Am 9: 350-7.

8. Blackburn N, Ziv I, Rang M. 1984. Correction of the malunited forearm fracture. Clin Orthop Relat Res 188: 54-7.

9. Jupiter JB, Ring D. 1996. A comparison of early and late reconstruction of malunited fractures of the distal end of the radius. J Bone Joint Surg Am 78: 739-48.

10. Athwal GS, Ellis RE, Small CF, Pichora DR. 2003. Computer-assisted distal radius osteotomy. J Hand Surg Am 28: 951-8.

11. Bilic R, Zdravkovic V, Boljevic Z. 1994. Osteotomy for deformity of the radius. Computer-assisted three-dimensional modelling. J Bone Joint Surg Br 76: 150-4.

12. Dobbe JG, Strackee SD, Schreurs AW, et al. 2011. Computer-assisted planning and navigation for corrective distal radius osteotomy, based on pre- and intraoperative imaging. IEEE Trans Biomed Eng 58: 182-90.

13. Rieger M, Gabl M, Gruber H, et al. 2005. CT virtual reality in the preoperative workup of malunited distal radius fractures: preliminary results. Eur Radiol 15: 792-7.

14. Schweizer A, Furnstahl P, Harders M, et al. 2010. Complex radius shaft malunion: osteotomy with computer-assisted planning. Hand (N Y) 5: 171-8.

15. Kunz M, Ma B, Rudan JF, et al. 2013. Image-guided distal radius osteotomy using patient-specific instrument guides. J Hand Surg Am 38:1618-24.

16. Vlachopoulos L, Schweizer A, Graf M, et al. 2015. Three-dimensional postoperative accuracy of extra-articular forearm osteotomies using CT-scan based patient-specific surgical guides. BMC Musculoskelet Disord 16: 336.

17. Walenkamp MM, de Muinck Keizer RJ, Dobbe JG, et al. 2015. Computer-assisted 3D planned corrective osteotomies in eight malunited radius fractures. Strategies Trauma Limb Reconstr 10: 109-16.

18. Ekblom AG, Laurell T, Arner M. 2014. Epidemiology of congenital upper limb anomalies in Stockholm, Sweden, 1997 to 2007: application of the Oberg, Manske, and Tonkin classification. J Hand Surg Am 39: 237-48.

19. Auerbach BM, Ruff CB. 2006. Limb bone bilateral asymmetry: variability and commonality among modern humans. J Hum Evol 50: 203-18.

20. Vroemen JC, Dobbe JG, Jonges R, et al. 2012. Three-dimensional assessment of bilateral symmetry of the radius and ulna for planning corrective surgeries. J Hand Surg Am 37: 982-8.

21. Gass T, Szekely G, Goksel O. 2014. Simultaneous segmentation and multiresolution nonrigid atlas registration. IEEE Trans Image Process 23: 2931-43.

22. Lorensen WE, Cline HE. 1987. Marching cubes: A high resolution 3d surface construction algorithm. SIGGRAPH Computer Graphics 21: 163–9.

23. Lüthi M, Jud C, Gerig T, Vetter T. 2016. Gaussian Process Morphable Models. arXiv preprint arXiv:1603.07254.

24. Umeyama S. 1991. Least-squares estimation of transformation parameters between two point patterns. IEEE Transactions on Pattern Analysis & Machine Intelligence 4: 376-380.

25. Jolliffe I. 2002. Principal component analysis. Wiley StatsRef: Statistics Reference Online.

26. Albrecht T, Lüthi M, Gerig T, Vetter T. 2013. Posterior shape models. Med Image Anal 17: 959-73.

27. Lachenbruch PA, Mickey MR. 1968. Estimation of error rates in discriminant analysis. Technometrics 10:1-11.

28. Hingsammer AM, Lazaros V, Dominik MC, Furnstahl P. 2015. Three-dimensional corrective osteotomies of mal-united clavicles--is the contralateral anatomy a reliable template for reconstruction? Clin Anat 28: 865-71.

29. Huttenlocher D, Klanderman G, Rucklidge W. 1993. Comparing images using the Hausdorff distance. IEEE Transactions on Pattern Analysis and Machine Intelligence 15: 850-63.

30. Letta C, Schweizer A, Furnstahl P. 2014. Quantification of contralateral differences of the scaphoid: a comparison of bone geometry in three dimensions. Anat Res Int 904275.

31. Schweizer A, Furnstahl P, Nagy L. 2013. Three-dimensional correction of distal radius intra-articular malunions using patient-specific drill guides. J Hand Surg Am 38: 2339-47.

32. Bindra RR, Cole RJ, Yamaguchi K, et al. 1997. Quantification of the radial torsion angle with computerized tomography in cadaver specimens. J Bone Joint Surg Am 79: 833-7.

33. Hollevoet N, Verdonk R. 2003. The functional importance of malunion in distal radius fractures. Acta Orthop Belg 69: 239-45.

34. Dumont CE, Thalmann R, Macy JC. 2002. The effect of rotational malunion of the radius and the ulna on supination and pronation. J Bone Joint Surg Br 84: 1070-4.

35. Fernandez DL. 2000. Should anatomic reduction be pursued in distal radial fractures? J Hand Surg Br. 25: 523-7.

TABLES

Table 1. Distances between the surfaces of the reconstructed and original (ground-truth) models using Euclidean and Hausdorff (HD) distance metrics.

Experiment	Average of Mean Distances (mm)	SD of Mean Distances (mm)	Average of HD Distances (mm)	SD of HD Distances (mm)
R_e	1.16	0.28	4.96	1.72
R_d	0.71	0.10	3.34	1.18
R_p	0.71	0.09	2.69	0.71
U_e	1.14	0.19	4.74	1.06
U_d	0.78	0.10	3.51	0.99
U_p	0.82	0.10	3.83	0.99

Table 2. Mean values and standard deviations (±) of the rotation and translation accuracy of the prediction.

	Rotation (°)			Translation (mm)		
	Pronation/ Supination	Flexion/ Extension	Ulnar-/ Radialduction	Proximal/ Distal	Radial/ Ulnar	Palmar/ Dorsal
R_e	6.5±5.2	2.5±1.8	1.7±1.4	3.0±2.4	0.8±0.6	1.0±0.7
R_d	2.9±2.2	0.6±0.5	0.5±0.4	1.0±0.8	0.5±0.4	0.6±0.5
R_p	4.0±3.1	0.4±0.3	0.5±0.3	0.8±0.7	0.6±0.4	0.6±0.4
U_e	6.7±4.8	2.1±1.6	1.9±1.4	2.0±1.6	0.9±0.6	1.1±0.8
U_d	4.7±3.8	0.8±0.6	0.7±0.6	1.3±0.9	0.7±0.5	0.8±0.6
U_p	2.4±1.9	0.3±0.3	0.3±0.2	0.6±0.4	0.4±0.4	0.5±0.4

The errors are given with respect to the axes of the anatomical coordinate system. Mean values and standard deviations were calculated from the absolute (unsigned) measurement values.

FIGURE LEGENDS

Figure 1:

Illustration of the leave-one-out experiments for radius, assuming that the ulna and the proximal radius are healthy in the experiment R_d. In the experiment R_p, the distal radius and the ulna are healthy. In the experiment R_e, only the ulna is considered healthy, and the all radius is considered pathological. The same experiments U_d, U_p, U_e were performed for the ulna, respectively.

Figure 2:

The fitted SSM are separated by a simulated osteotomy plan (A and C for configuration U_e and R_d, respectively), and aligned to the ground-truth surface (B and D). The relative transformation of the separated parts between their predicted (A and C) and ground-truth position (B and D) was then used as the error measure.

Figure 3:

Representation of the anatomical coordinate system for radius (A) and ulna (B). Rotation around the x-axis (red) corresponds to a correction in the transverse plane (pronation/supination), rotation around the y-axis (green) in the sagittal plane (flexion/extension), and z-axis (blue) in the frontal (ulnar-/radialduction). The coordinate system was adapted in that way that a positive rotation around the defined axis defined for both sides of the radius and ulna a supination, flexion and radialduction, respectively.

Figure 4:

Box-plots showing the accuracy of the prediction (signed) of the SSM with respect to (A) rotation error of the radius, (B) rotation error of the ulna, (C) translation error of the radius, and (D) translation error of the ulna. The errors are given with respect to the axes of the anatomical coordinate system.

Figure 5:

Box-plots showing the accuracy of the prediction (unsigned) of the SSM with respect to (A) rotation error of the radius, (B) rotation error of the ulna, (C) translation error of the radius, and (D) translation error of the ulna. The errors are given with respect to the axes of the anatomical coordinate system.

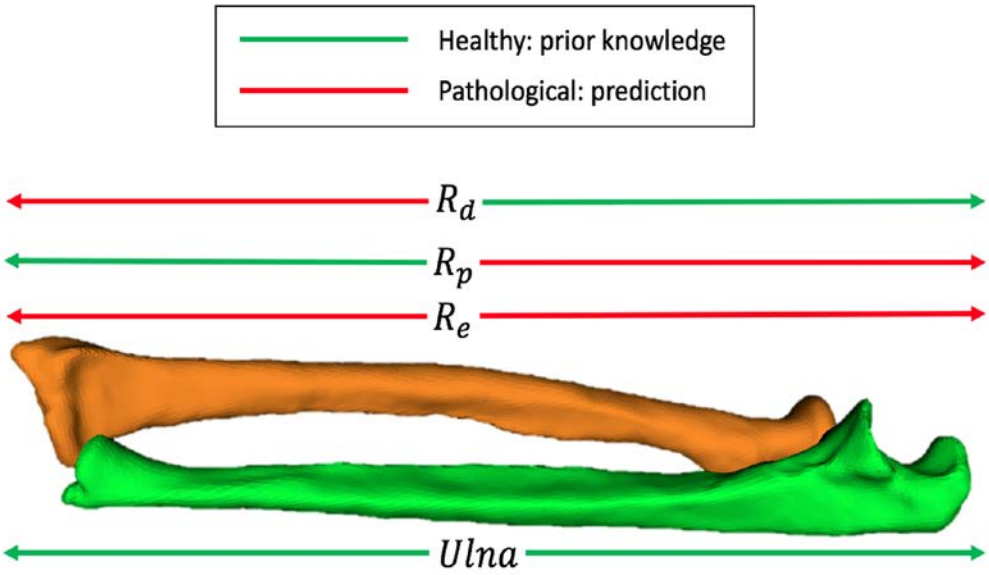

Figure 1

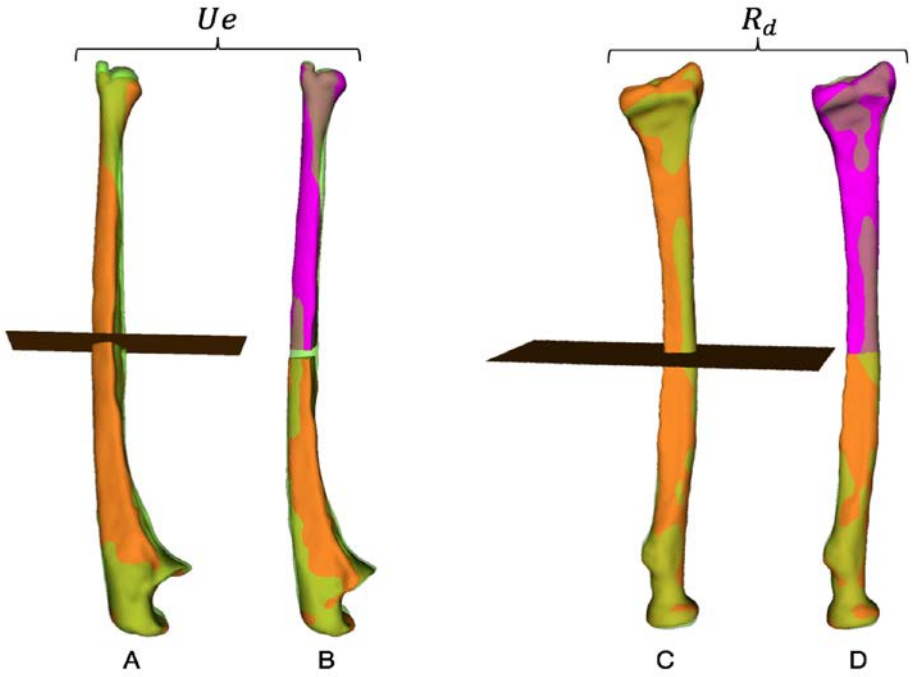

Figure 2

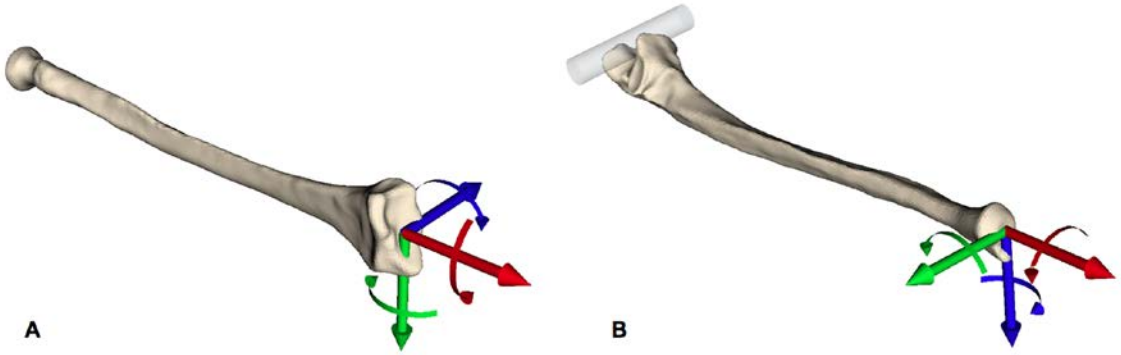

Figure 3

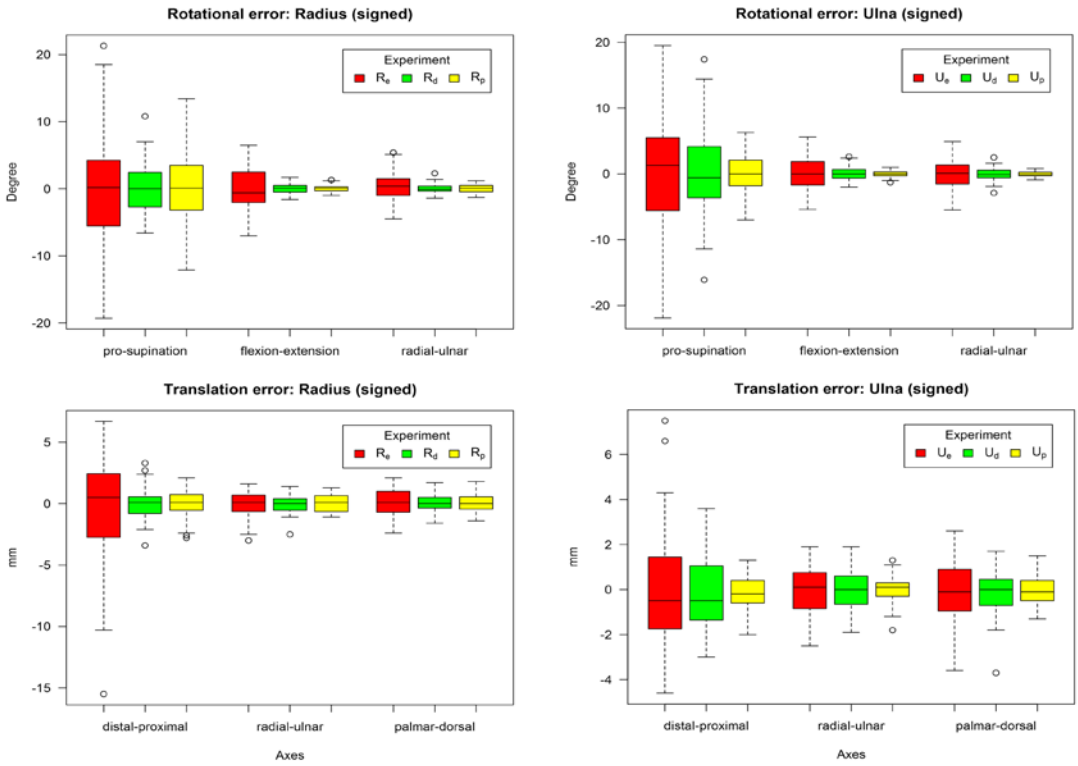

Figure 4

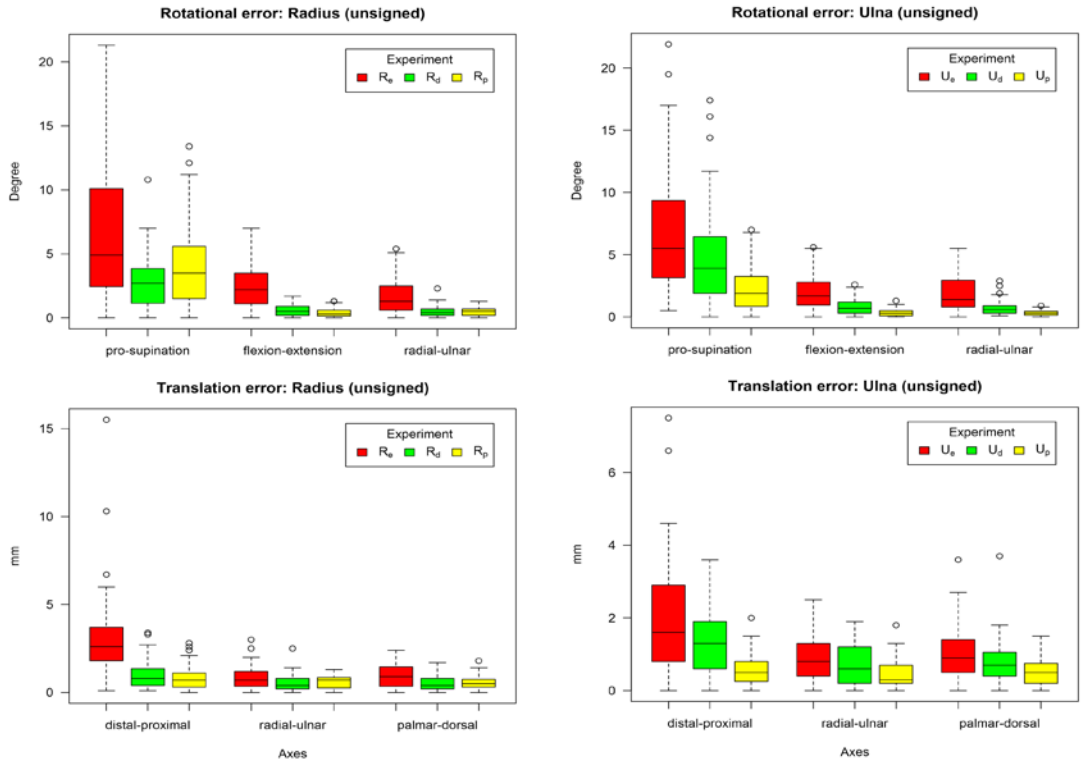

Figure 5